

Efavirenz dissolution enhancement V – A combined top down/bottom up approach on nanocrystals formulation

Gabriela Julianelly Sartori^{1*}, Livia Deris Prado^{2,3},
Helvécio Vinícius Antunes Rocha^{1,2}

¹Programa de Pós-Graduação Profissional em Gestão, Pesquisa e Desenvolvimento na Indústria Farmacêutica / Farmanguinhos / Fiocruz / Rio de Janeiro / Rio de Janeiro / Brasil, ²Laboratório de Micro e Nanotecnologia / Farmanguinhos / Rio de Janeiro / Rio de Janeiro / Brasil, ³Programa de Pós-Graduação em Química / Universidade Federal Fluminense / Niterói / Rio de Janeiro / Brasil

Efavirenz is one of the most commonly used drugs in HIV therapy. However the low water solubility tends to result in low bioavailability. Drug nanocrystals, should enhance the dissolution and consequently bioavailability. The aim of the present study was to obtain EFV nanocrystals prepared by an antisolvent technique and to further observe possible effect, on the resulting material, due to altering crystallization parameters. A solution containing EFV and a suitable solvent was added to an aqueous solution of particle stabilizers, under high shear agitation. Experimental conditions such as solvent/antisolvent ratio; drug load; solvent supersaturation; change of stabilizer; addition of milling step and solvents of different polarities were evaluated. Suspensions were characterized by particle size and zeta potential. After freeze-dried and the resulting powder was characterized by PXRD, infrared spectroscopy and SEM. Also dissolution profiles were obtained. Many alterations were not effective for enhancing EFV dissolution; some changes did not even produced nanosuspensions while other generated a different solid phase from the polymorph of raw material. Nevertheless reducing EFV load produced enhancement on dissolution profile. The most important modification was adding a milling step after precipitation. The resulting suspension was more uniform and the powder presented greater enhancement of dissolution efficacy.

Keywords: Efavirenz. Particle size. Nanocrystals. Anti-solvent precipitation. Dissolution. Nanocrystallization.

INTRODUCTION

Efavirenz (EFV) is a non-nucleoside inhibitor of HIV reverse transcriptase, an antiretroviral drug used widely in anti-AIDS therapy (Burger *et al.*, 2006). The bioavailability of EFV tablets is between 40% and 45%. Clinical studies show that the bioavailability of the liquid form is 20% lower than that of the solid form and has high variability between the starved and fed states (Chiappetta *et al.*, 2010). EFV is a crystalline powder with

a low water solubility of 3-9 µg/mL and a low intrinsic dissolution rate (IDR) of 0.037 mg.cm⁻².min⁻¹. According to the Biopharmaceutics Classification System (BCS), EFV is defined as a class II drug, meaning it has low solubility and high permeability (Chiappetta *et al.*, 2010; Cristofolletti *et al.*, 2013; Patel *et al.*, 2014).

The most common enhancement technique to increase the dissolution rate of a drug is particle size reduction to the micrometric scale (Cho *et al.*, 2010; Khadka *et al.*, 2014; Savjani, Gajjar, Savjani, 2012). However, for drugs with very low water solubility, such as EFV, it can be very promising to reach the nanometric scale (Fandaruff *et al.*, 2014; Muller, Keck, 2004). Drug nanocrystals are more commonly used than other nanotechnology approaches

*Correspondence: G. J. Sartori. Instituto de Tecnologia em Fármacos - Farmanguinhos. Av. Comandante Guarany, 447, Jacarepaguá, Rio de Janeiro, Brasil. CEP: 22775-903. Phone: 55 21 982951582. E-mail: gabrielajsartori@gmail.com

in the pharmaceutical market (Gao *et al.*, 2013). Drug nanocrystals are crystalline particles dispersed in an organized crystal arrangement with an average diameter smaller than 1000 nm (Patel *et al.*, 2011). Nanocrystals are generally considered a safe structure to enhance the bioavailability of low water-soluble drugs (Gao *et al.*, 2012).

The methods used to prepare nanocrystals can be divided into two categories: bottom-up and top-down. The bottom-up techniques consist of dissolving the drug in a solvent system and then transforming this solution into an antisolvent environment (Verma, Gokhale, Burgess, 2009). The driving force of crystal formation is supersaturation, which is why these methods are also known as precipitation methods (de Waard *et al.*, 2009). Of all the available techniques for nanocrystal preparation, antisolvent precipitation was chosen for this study.

A brief review of the published literature about EFV nanocrystals includes a nanosuspension prepared by a modified antisolvent method (Jain *et al.*, 2013), the preparation of nanocrystals by pearl milling (Patel *et al.*, 2014), and a preparation method combining a modified antisolvent precipitation procedure with hot melt extrusion (Ye *et al.*, 2015). Overall, these studies propose complex procedures, with several long steps, which could present some problems during scaling up. Another important issue is that the resulting nanosuspensions have low drug loads. Therefore, the development of an EFV nanocrystal preparation method that combines the simplicity of nanocrystallization with a high drug load is still needed.

Many criteria can affect the outcome of this technique, especially those related to the crystallization kinetics (such as supersaturation degree) and those related to particle size and growth (such as stabilizer concentration) (Sinha, Müller, Möschwitzer, 2013a). Another factor vital to ensuring a uniform size distribution is agitation. The homogenizing process influences the nucleation rate and can lead to a more adequate size distribution of the crystals (Liu *et al.*, 2012; Matteucci *et al.*, 2006).

The present article follows previous work (da Costa *et al.*, 2015; da Costa *et al.*, 2013; Hoffmeister *et al.*, 2017; Sartori, Prado, Rocha, 2017) that investigated ways to enhance EFV dissolution by developing a new medicine with greater and more reproducible dissolution/bioavailability. A previous study has already shown good

prospects for the nanocrystal approach, using cavitation as a stirring method (Sartori, Prado, Rocha, 2017). In this same study, several experimental parameters were tested until a promising sample was found.

Nevertheless, when ultrasound waves are applied to a liquid as a stirring method, they result in the formation and collapse of bubbles. This process produces a cyclic succession of expansion and compression phases (Wu *et al.*, 2011). The mechanical vibration derived from this phenomenon generates enormous local heating (Flint Suslick, 1991); hence, there is a possibility of drug instability or scale-up difficulties. Therefore, there is a need to develop a low-energy method for nanocrystal preparation.

The aim of the present paper is not only to determine the effects of changing the homogenizing technique from the ultrasound technique used in previous studies (Sartori, Prado, Rocha, 2017) to a rotor-stator agitation but also to observe the consequences of modifications of the experimental conditions on the dissolution profile of EFV nanocrystals, especially the addition of a milling step (top-down technique) to prevent particle growth.

MATERIAL AND METHODS

Material

EFV was purchased from two different suppliers, which cannot be disclosed because of confidentiality issues. Ethanol, acetonitrile, acetone and methanol (analytical degree) were purchased from Tedia; hydroxypropyl methylcellulose (HPMC) E5 was purchased from Colorcon; polyvinyl pyrrolidone (PVP) K30 was purchased from Boai NKY; sodium lauryl sulphate (SLS) was purchased from VETEC.

Methods

Nanocrystal preparation

For the formation of EFV nanosuspensions, it was necessary to prepare two different solutions. The first one, the solvent phase, comprised the drug dissolved in methanol. The second solution contained stabilizers dissolved in deionized water. The electrostatic stabilizer

used in all preparations was SLS at a concentration of 2% (w/w), and the steric stabilizers used were HPMC and PVP at a concentration of 40% (w/w), related to the EFV mass used, at room temperature. In some samples, different experimental conditions were tested, and the rationale for the preparation of samples and the conditions

tested in those experiments are outlined as a workflow in Figure 1. In TX2, the solvent/antisolvent ratio was 1:1 (the ratio in other samples was 1:9); in TX4, the influence of a low-temperature antisolvent solution was evaluated, and sample TX7 was passed through a Meteor model REX 1-K/B90-52 colloid mill (Table I).

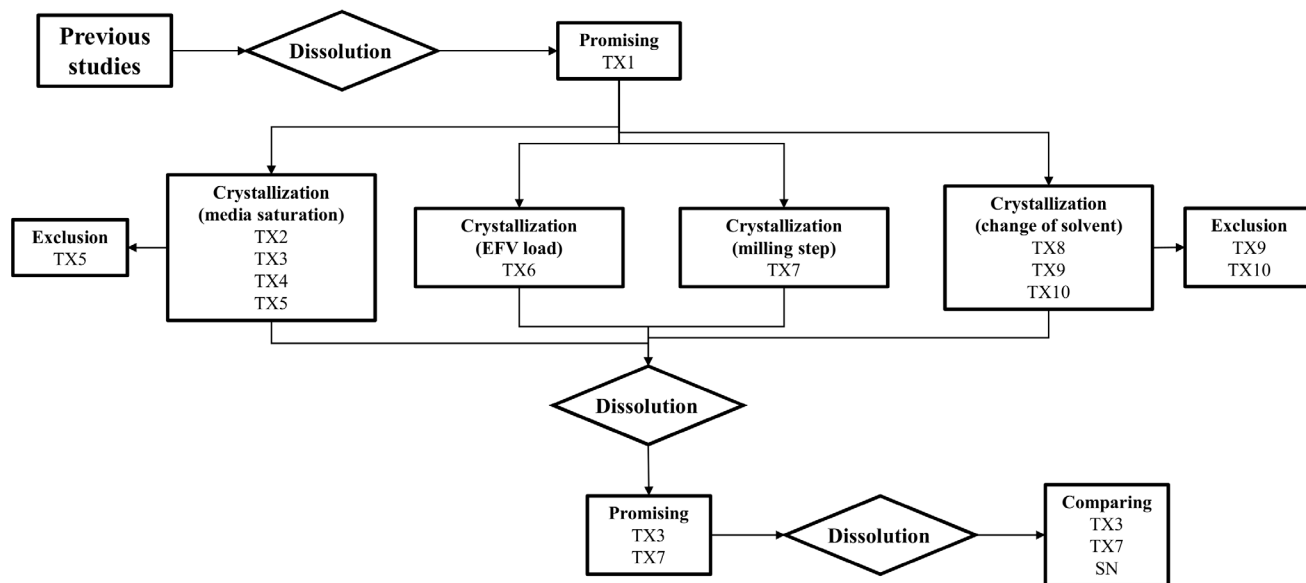


FIGURE 1 - Workflow for the design of the different formulations.

Efavirenz (EFV) nanocrystallization experiments presented step-by-step. Samples were considered promising or excluded based in the dissolution assay, hence this test was in a diamond

TABLE I - Experimental parameters used in the preparation of the samples

Sample	EFV	SLS	Polymer		Special parameters
	(% w/v)	(%w/w)	Type	(%w/w)	
TX1	53.33	2	HPMC E5	40	
TX2	8.00	2	HPMC E5	40	Solvent/antisolvent ratio 1:1
TX3	13.35	2	HPMC E5	40	
TX4	13.35	2	HPMC E5	40	Antisolvent temperature between 7.2 – 7.5 °C
TX5	70.00	2	PVP K30	40	
TX6	10.00	2	PVP K30	40	
TX7	13.35	2	HPMC E5	40	After crystallization went through to colloid milling for 1 hour
TX8	13.35	2	HPMC E5	40	Solvent: Ethanol
TX9	13.35	2	HPMC E5	40	Solvent: Acetone
TX10	13.35	2	HPMC E5	40	Solvent: Acetonitrile

Note: Efavirenz (EFV); Sodium Lauryl Sulphate (SLS)

The solvent solution was added to the antisolvent phase under vigorous agitation by an Ultra-turrax IKA model T25 at 20 000 RPM, and this agitation was maintained for one minute. The resulting suspension was freeze-dried using a BETA 1-16 Christ freeze-dryer to obtain a powder.

Particle size and zeta potential analysis

The particle size and zeta potential (ζ) were evaluated by dynamic light scattering (DLS) using a Nano ZS90 Malvern Zetasizer equipped with He-Ne LASER ($\lambda = 633$ nm) and a detector fixed at a 90° angle. Aliquots of the suspensions, taken immediately after preparation, were diluted to approximately 0.1% (v/v) in deionized water at room temperature. The zeta potential was measured by determining the electrophoretic mobility of the suspension using the Smoluchowski equation (Sze *et al.*, 2003).

Powder X-ray diffraction

The analyses were performed on a D8 Advance Bruker diffractometer equipped with a LYNXEYE XE detector at room temperature using Cu-K α ($\lambda=1.5418$ Å) radiation; the voltage and current during the assay were 40 kV and 40 mA, respectively, with a step size of 0.02° and a step time of 0.01 second. Powder samples, placed in the appropriate support, were scanned from 4° to 40° . Samples TX4, TX6 and TX7 also underwent a second analysis using the same parameters except with a step time of 0.5 second.

Infrared spectroscopy

The samples were analysed with a Nicolet 6700 Thermo-Nicolet infrared spectrometer equipped with OMNIC 7.0 software, with small amounts of the samples deposited directly in the attenuated total reflectance (ATR) accessory. The spectra were registered from 4000 to 600 cm^{-1} with 4 cm^{-1} resolution and 32 scans.

Scanning electron microscopy

The samples were spread on a sample holder and then coated with gold by an SCD 050 Sputter BalTech

coater. The particle morphology of each sample was observed at several magnifications ranging from 500 to 30000 times using Quanta 400 FEI and TM3030Plus Hitachi scanning electron microscopes.

Sample dosing (drug assay)

The samples were dissolved in methanol to produce a primary solution with a concentration of 1 mg/mL. The primary solution was then diluted to enable the analysis with a UV-1800 Shimadzu spectrophotometer at a λ of 248 nm. The EFV content of each sample was calculated using a previously obtained analytical curve.

Dissolution profile

The dissolution test was conducted according to the Farmacopeia Brasileira 5th edition (Brasil, 2010) paddle method using an Evolution 6000 Distek dissolution instrument. The temperature of the medium was maintained at 37°C , and the sample was stirred at a constant stirring rate of 50 rpm. A sample with a mass corresponding to 100 mg of efavirenz, calculated based on sample dosing, was dispersed in 900 mL of medium containing an aqueous 0.1% (w/v) SLS solution; 11 mL samples were drawn at 5, 10, 15, 20, 25, 30, 45, 60 and 90 minutes. Sink conditions were maintained during the entire assay. The drug content was determined using a UV-1800 Shimadzu spectrophotometer at 248 nm, based on a previously obtained calibration curve. The dissolution profiles were compared two-by-two using ANOVA with Microsoft Excel® software. According to this statistical test, all dissolution profiles present significant differences from each other, and the dissolution efficiency was also calculated.

RESULTS AND DISCUSSION

Nanocrystal preparation

Initial crystallization conditions

Previous crystallization studies evaluated EFV solubility in different solvents and at several stabilizer

concentrations (data not shown). The most promising sample is labelled TX1 and contains 40% HPMC and 2% SLS. Hence, this sample was chosen as the base formulation from which other experiments were derived.

Ultra-turrax samples generate foam during and just after preparation, especially at the top of the beaker, which is possibly related to the high concentration of SLS and to the agitation method. The bottom part of the suspension was similar to a clustered thick paste.

From a production point of view, suspensions were not favourable, since they could hinder nanosuspension handling. Therefore, a less viscous suspension would be more suitable for processing.

Changing the solvent/antisolvent ratio

It is expected that a greater volume difference between the solvent and antisolvent phases will result in a higher nucleation rate and, therefore, a smaller particle size (Sinha, Müller, Möschwitzer, 2013b; Zhao *et al.*, 2007). TX1 was prepared using a solvent/antisolvent ratio of 1:9; sample TX2 used a ratio of 1:1.

The resulting suspensions were similar to a very thick paste and did not disperse in water. After drying, the resulting powder was characterized.

Drug load reduction

To enhance the mixing efficiency by reducing the system viscosity, two samples were prepared by decreasing the EFV drug load. Sample TX3 maintained the antisolvent at room temperature, while TX4 maintained the antisolvent solution only between 7.0 and 7.5 °C, which was achieved by applying an ice bath.

The TX3 sample was foamy and viscous, while TX4 was milky and fluid. Sample TX4 also presented visible sedimentation, but no visible large particles were observed.

Particle size analysis of sample TX4 shows that the most significant particle population has an average diameter of 222.6 nm. However, a second peak representing micrometric particles was also observed (Table II). This second population could be related to the sediment particles, since this sample had visible sedimentation or even particle aggregation. The polydispersity index (PDI) is lower than 0.5, indicating a uniform distribution. The zeta potential (ζ) indicates the stability of suspensions. The optimum value of the zeta potential for suspensions with steric and electrostatic stabilization is greater than ± 20 mV (Liu *et al.*, 2012). Sample TX4 presented an absolute value of ζ higher than ± 20 mV, which is considered adequate. Both PDI and ζ are parameters related to the physical stability of the suspension (Sawant *et al.*, 2011; Wu, Zhang, Watanabe, 2011). Because sample TX3 did not disperse in water, DLS analysis was not possible.

TABLE II - Relation of particle size and zeta potential analysis

Sample	Medium diameter (nm)			PDI	Zeta potential (mV)
	Peak 1	Peak 2	Peak 2		
TX4	222.6	5440		0.419	-37.6
TX5	1756	170.6	4863	0.857	-55.7
TX6	182.2	550.2	5306	0.408	-57.6
TX7-before	210.5	840.4	4737	0.431	-28.7
TX7-after	491.9	5429	-	0.389	-29.2
TX9	960.6	5378	174.2	0.652	-29.5
TX10	768.7	4526	-	0.639	-3.74

Note: Polydispersity Index (PDI)

Solvent supersaturation

There is a relationship between a high degree of saturation and intensification of the nucleation rate (Sinha, Müller, Möschwitzer, 2013a). Hence, sample TX5 was prepared using a supersaturated solution of EFV in methanol as the solvent phase. The suspension had a thick and clustered appearance; however, the TX5 suspension was dispersible in water, so DLS was possible.

Table II presents the particle size distribution of TX5. Three different peaks can be observed. Peak 1 is more intense than the other peaks and is attributed to particles with an average diameter larger than 1 μm ; peak 2 indicates a second particle population with an average diameter of 170.6 nm, and peak 3 is attributed to even larger micrometric particles. Accordingly, the PDI obtained was very high, reflecting the low uniformity of particles in the suspension.

Although TX5 presented an adequate ζ , the particle size analysis indicates that the supersaturation condition was not the most favourable for nanocrystal formation. As a result, TX5 was not subjected to the characterization and dissolution tests.

Change in the steric stabilizer

A brief literature review revealed studies using EFV and PVP (Alves *et al.*, 2014; Jain *et al.*, 2013; Patel *et al.*, 2014), and since the efficacy of these polymers as steric stabilizers has already been tested in other nanocrystallization methods by this group, sample TX6 was prepared using the same experimental conditions used to prepare TX3, but the polymer used was PVP K30.

The suspension had a fluid nature; however, after some time, it was possible to observe large aggregate formation. DLS analysis (Table II) exhibited peaks 1 and 2 corresponding to particles with average diameters of 182 nm and 550.2 nm, respectively. Since both peaks have nanometric dimensions, the sample PDI was lower than 0.5. The zeta potential of -57.6 mV is considered suitable, indicating good physical stability.

Adding a milling step after crystallization

It has been reported in the literature that a bottom-up preparation can be followed by a top-down technique to prevent particle growth (Salazar *et al.*, 2012; Yang *et al.*, 2016). Sample TX7 was prepared using the same conditions used to prepare TX3; however, a milling step was added immediately after precipitation. The mechanical stress generated by particle collision inside the mill is expected to prevent particle growth (Carstensen, 2001).

After one hour of milling, a reduction in the viscosity was observed. The initial appearance was the same as that of TX3, and the foam, which was initially only on the top of the suspension, was observed throughout the whole suspension.

To verify the suspension stability, a particle size DLS analysis was performed before and after the milling step. Peak 1 in the data for TX7 before and after milling was observed at 210.5 nm and 491.9 nm, respectively (Table II).

There was also a reduction in the PDI after the milling process (Table II), indicating that this step produces more uniform suspensions. Although some growth has been detected, the particles are still within the nanoscale range, indicating that milling is effective in preventing significant particle growth. The zeta potentials of both suspensions were similar and considered adequate for a stable suspension.

Changing the solvent

With drugs of very low solubility, such as EFV, the use of a less polar solvent should result in more effective interaction between the drug and the stabilizers and a higher nucleation rate (Beck, Dalvi, Dave, 2010; Sinha, Müller, Möschwitzer, 2013a). Thus, smaller particles should be obtained.

Three new samples (TX8, TX9 and TX10) were prepared using ethanol, acetone and acetonitrile, respectively; the conditions used to prepare TX3 were applied. The suspensions were reasonably viscous and presented visible particles; they also presented phase separation, forming one slightly turbid liquid and a dense

foam. Only TX9 and TX10 dispersed in water and were subsequently subjected to DLS analysis.

The DLS data for samples TX9 and TX10 exhibited peak 1 related to particles with an average diameter close to 1 μm ; peak 2 corresponding to particles larger than 4 μm was also observed. Both samples had PDI values greater than 0.5. Sample TX10 had a ζ potential of -3.74 mV, which is considered low for particle stabilization. Although TX9 had a ζ potential of -29.5 mV, particle analysis proved that this sample was not a nanosuspension. Considering the unsatisfactory results for TX9 and TX10, these samples were discarded.

Solid state characterization

All samples considered promising were freeze-dried and characterized by SEM, infrared spectroscopy and PXRD. The samples were TX1, TX2, TX3, TX4, TX6, TX7 (after milling) and TX8.

Particle morphology

Photomicrographs of the processed samples and raw EFV exhibit a modified particle morphology. The active pharmaceutical ingredient (API) is composed of rough micrometric particles. Overall, the samples exhibit gel formation or long needle-shaped particles (Figure 2).

Sample TX1 presented more intense gel formation than did TX2, displaying large aggregates formed by smaller elongated particles with a nanometre-scale width. It is possible that the gelation in TX2 is not as intense as that in TX1 because a smaller volume of water was used during the preparation. Another hypothesis is that the great amount of methanol utilized could prevent the formation of the HPMC gel (Nickerson *et al.*, 2009).

Film formation was also observed in samples TX3 and TX4, which both contain the same polymer concentration as TX2. This reinforces the idea that the methanol/water ratio is related to this phenomenon. Evidently, the film in TX3 is more uniform than that in TX4. This may be due to deformations that occurred during the freezing step of the freeze-drying process (Lee, Cheng, 2006), which makes clear the need for a specific study of the drying method.

Sample TX6 shows elongated particles of nanometric width, as well as aggregates and thicker particles, in accordance with the DLS analysis. The TX6 morphology demonstrates significant particle growth, indicating that PVP may not be an ideal steric stabilizer for this preparation method.

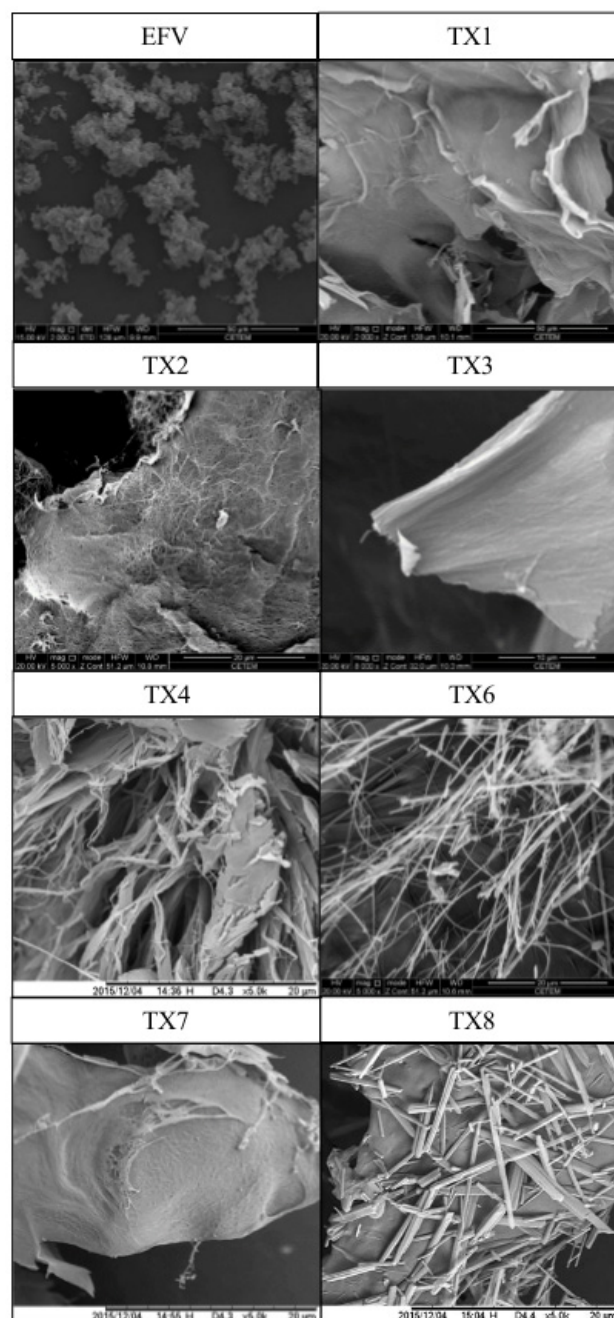


FIGURE 2 - Photomicrographs from SEM analysis.

Pictures of different samples, obtained through microscopy analysis. In general samples presented needle shape particles with nanometric width

Sample TX7 also presented intense film formation, and TX8 was composed of large agglomerates of several sizes. With a more accurate analysis, it was observed that the aggregates are formed by long and fine particles. This indicates that the conditions used are not favourable for preparing nanocrystals, in conflict with the literature (Beck *et al.*, 2010; Sinha, Müller, Möschwitzer, 2013a). Although fine elongated particles were generated, it is shown that they tend to aggregate, implying that the same preparation conditions were not effective for suspension stabilization when the solvent was ethanol.

Infrared spectroscopy.

The infrared spectra of the samples and API (Figure 2) present all the bands associated with the EFV

functional groups (Gomes *et al.*, 2013). This indicates not only that EFV is present in the samples but also that no chemical reaction occurs between the drug and the stabilizers, due to some kind of incompatibility.

The high polymer concentration in the samples reduces the EFV proportion in the bulk, leading to a decrease in the signal intensity; this effect is more evident in TX3 than in other samples (arrow in Figure 2). Another possibility is that the lactam portion of the EFV molecule forms hydrogen bonds with the polymer, thereby reducing the vibration and intensity of absorption (Stuart, 2004). A common effect of particle comminution by this method is the reduction of the crystalline domain, which tends to decrease the infrared absorption of crystalline powders (Shankar, Rhim, 2016).

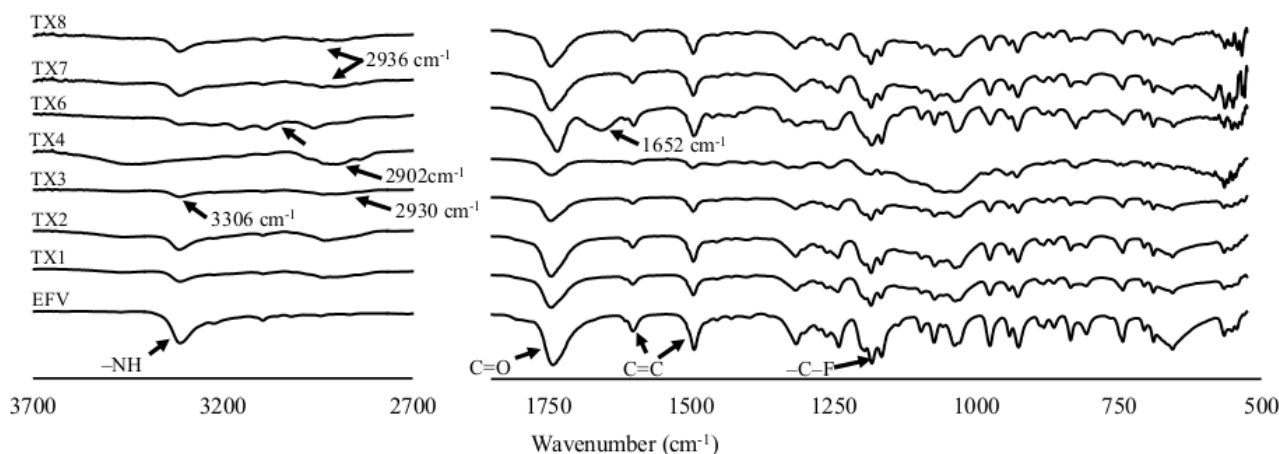


FIGURE 3 - Infrared spectra of EFV and processed samples.

Efavirenz (EFV) respective group bands are marked with arrows. Subsequent arrows are marking: 2902 cm^{-1} , 2930 cm^{-1} and 2936 cm^{-1} are relative to CH and CH_2 bands; 1652 cm^{-1} associated with the pyrrolic ring of the PVP;

Samples TX3 and TX4 presented bands at 2930 cm^{-1} and 2902 cm^{-1} , respectively, which are not characteristic of EFV molecules. These bands are commonly associated with CH and CH_2 (Stuart, 2004), probably indicating the presence of a polymer. Steric stabilization of TX6 is achieved by PVP, and the infrared spectrum of this sample has a band at 1652 cm^{-1} associated with the pyrrolic ring of the polymer (Laot, 1997). Overlapping of the bands in the range between 2860 and 3304 cm^{-1} was detected.

The presence of hydrogen bonds reduces the vibration of amine, amide and hydroxyl groups, reducing the intensity or wavenumber of the bands related to these functional groups (Theophile, 2012). The inflexibility of the hydrogen bonds formed between EFV and PVP masks the NH band (arrow in Figure 2). The spectra of samples TX7 and TX8 have a band of 2936 cm^{-1} , usually associated with alkane CH bonds (Stuart, 2004), which is possibly related to the presence of a high concentration of HPMC.

Powder X-ray diffraction

According to the diffraction patterns presented in Figure 3a, samples TX1, TX2, TX3 and TX8 maintained crystalline characteristics after precipitation. It is possible to identify EFV polymorph I, especially by the peak at $2\theta=6.2^\circ$ (Mahapatra *et al.*, 2010). Moreover, an increase in the peak width can be observed, possibly related to the reduction in the crystalline domain that is usually associated with particle size reduction (Blachère, Brittain, 2008), in accordance with the infrared analysis.

Sample TX7 presents a halo indicating the presence of amorphous EFV resulting from the

preparation method (Blachère, Brittain, 2008). For a more meticulous investigation, samples TX4, TX6 and TX7 underwent a new PXRD assay, increasing the step time to enhance the signal intensity (Blachère, Brittain, 2008).

The pattern obtained for samples TX4 was compared with the calculated patterns of other polymorphs of EFV (data not shown); however, no clear resemblance was found. In a study of the thermodynamic relations between several EFV polymorphs (Chadha *et al.*, 2012), a crystalline form was found by slow recrystallization from hexane, with a diffraction pattern similar to that of TX4 (Figure 3b).

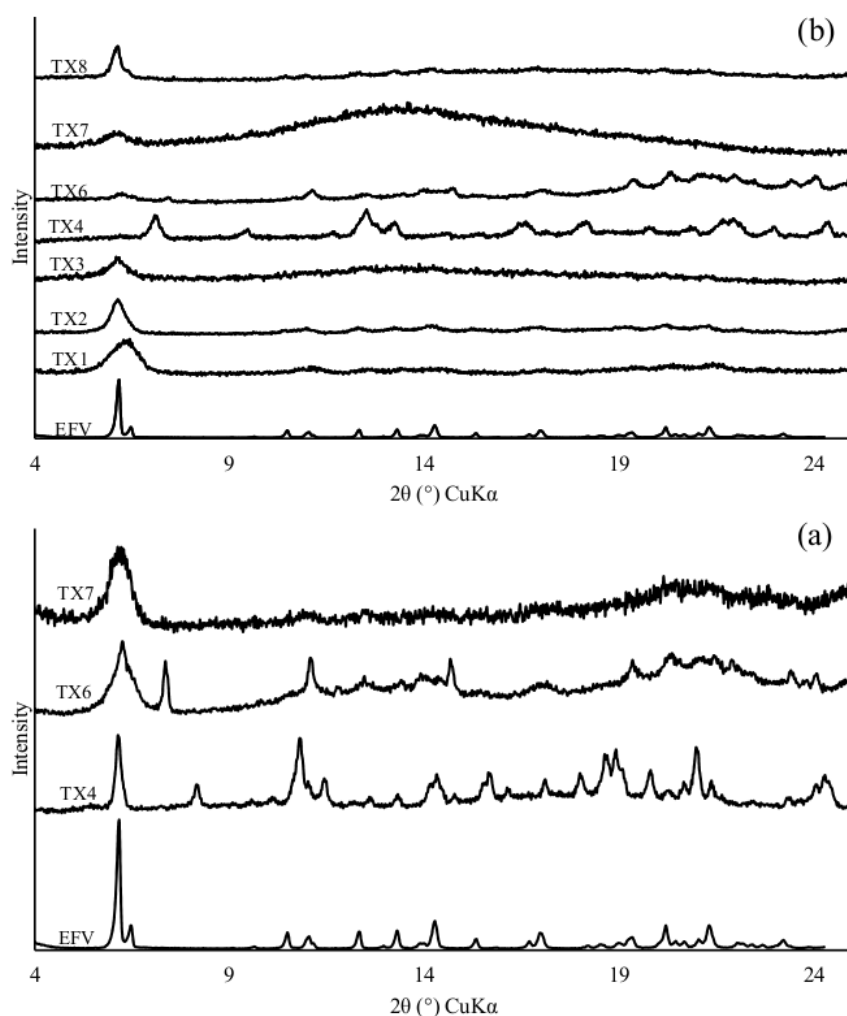


FIGURE 4 - (a) Diffraction patterns using step time of 0.01 seconds; (b) Diffraction patterns using step time of 0.5 seconds. Comparison of diffraction patterns of samples with efavirenz (EFV), showing the presence of peaks relative to efavirenz polymorph I.

In a new PXRD analysis of TX6, it was possible to confirm the presence of EFV form I, but still some preferential orientation can be observed (Blachère, Brittain, 2008). Increasing the step time reduces the noise associated with the diffraction pattern, so it is possible to detect form I with $2\theta=6.2^\circ$ in sample TX7.

Dissolution

Observing the dissolution profiles (Figure 4) and dissolution efficiency calculated for each sample (Table III) suggests that all samples, with the exception of TX2, TX6 and TX8, presented enhanced dissolution profiles. Sample TX2 has the lowest dissolution profile, even in

comparison with the drug itself. This result was expected, since modification of the solvent/antisolvent ratio could significantly reduce the saturation degree of the system, favouring crystal growth. Hence, the dissolution profile is in accordance with theory.

Sample TX6 uses PVP as a steric stabilizer, as mentioned in the EFV-related literature. Nevertheless, the physical characterization and dissolution profile indicated that this modification was not beneficial. The low dissolution profile of sample TX8 is not in agreement with the literature since the use of a less polar solvent, when crystallizing a drug with very low water solubility such as EFV, should increase the nucleation rate (Beck, Dalvi, Dave, 2010).

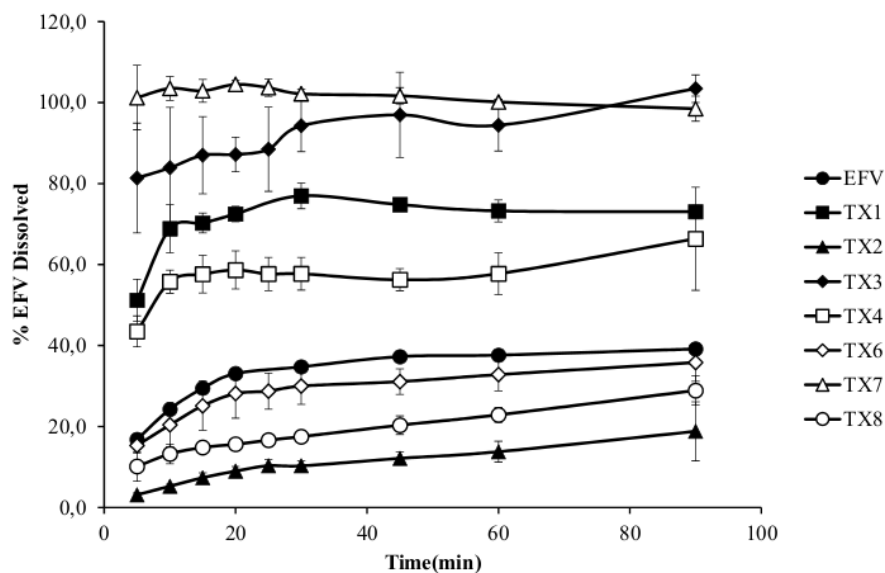


FIGURE 5 - Dissolution profiles of samples.

Dissolution profiles of samples compared with efavirenz, pointing that the use of the technique was efficient in enhancing dissolution.

TABLE III - Drug concentration and dissolution efficiency of each sample in % with the respective standard deviation (SD)

Samples	EFV content (% average \pm SD)	Dissolution efficiency (% average \pm SD)
TX1	57.19 \pm 3.55	70.26 \pm 1.39
TX2	57.46 \pm 2.21	11.70 \pm 2.30
TX3	55.67 \pm 4.01	91.25 \pm 3.98
TX4	58,30 \pm 3.52	56.47 \pm 4.90
TX6	48.94 \pm 5.30	29.23 \pm 4.00
TX7	61.17 \pm 3.23	98.41 \pm 1.07
TX8	63.46 \pm 7.51	19.79 \pm 1.52

Note: Efavirenz (EFV)

Samples TX3 and TX4 have the same formulation, with their main difference being the antisolvent temperature used in their preparation. Due to the higher degree of saturation promoted by the low antisolvent temperature, it was expected that TX4 has a greater dissolution enhancement than TX3 (Sinha, Müller, Möschwitzer, 2013b). However, by maintaining the antisolvent at room temperature in conjunction with EFV mass reduction, sample TX3 presented a more positive effect towards dissolution profile enhancement.

As TX4 has a different crystalline structure than TX3, this can affect several physicochemical properties, and thus, a more accurate study may be conducted in

the future. Among all samples, the one that achieved the highest dissolution was TX7, proving that the addition of a milling step was able to prevent particle growth and produce a uniform suspension, the particles maintained their stability through freeze-drying, and the obtained EFV nanocrystals presented a high dissolution profile.

Comparison with the sonication method

A comparison of the dissolution profiles of samples TX3 and TX7, the most promising formulations, with the profile of a sonication sample (SN11) from a previous study (Sartori, Prado, Rocha, 2017) with the best improvement and EFV is presented in Figure 5.

In general, the samples prepared by rotor-stator agitation were more viscous, similar to a paste, while the sonicated samples were more fluid. In a supersaturated environment, crystallization tends to occur. It has been reported that mass transfer from solution to the solid phase could be compromised due to the high viscosity of the suspension (Tung *et al.*, 2008).

However, it is well known that in a suspension, particles are in Brownian motion, which is more intense in the case of more fluid environments, increasing particle collisions with subsequent growth (Comba, Sethi, 2009). Therefore, increasing the viscosity is an alternative to improve the stability of a highly concentrated suspension (Peltonen, Hirvonen, 2010).

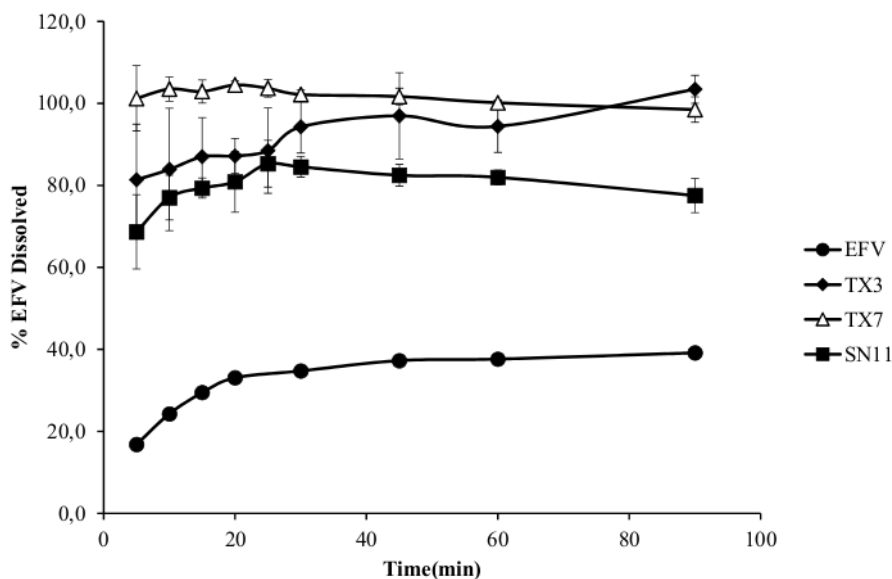


FIGURE 6 - Comparison between dissolution profiles of samples TX3, TX7, EFV and sonication sample (SN11). Comparison of dissolution profiles of the most promising samples with efavirenz and sample SN11 (from previous)

Thus, TX3 and TX7 exhibit greater dissolution than SN11. However it is important to emphasize that suspension viscosity is a property to optimize, not maximize, and that the determined level should not be exceeded, which would hinder the crystallization process.

From a production point of view, the higher enhancement of nanocrystals prepared by a high shear-based technique can be considered positive. Since cavitation-based techniques are more expensive and generate intense heat, the use of rotor-stators is more suitable when developing a low-cost and easy-to-scale up process.

CONCLUSION

Early attempts to crystallize TX1 were promising, as confirmed by dissolution enhancement, and they were used to establish a basic formulation. Changing the solvent/antisolvent ratio and the kind of solvent did not produce satisfactory results, and the sample had the lowest dissolution profile. Reducing the antisolvent temperature leads to the formation of a different crystalline state, possibly impairing dissolution. Changing the solvent also resulted in unsatisfactory outcomes.

Reducing the mass of EFV in TX3 produced a sample with one of the highest levels of dissolution. Sample TX7

exhibited higher dissolution than turrax samples and previous samples prepared using sonication, confirming that the addition of a milling step after crystallization is an interesting alternative to prevent growth.

Suspensions prepared by sonication were less viscous than those prepared with high shear. However, the dissolution percentage was higher for the latter samples (when compared with those prepared by sonication). The addition of a milling step produced a suspension that was more viscous than those prepared with sonication but not as pasty as the other samples that did not pass through the colloidal mill.

As a result, the combination of bottom-up (antisolvent precipitation) and top-down (colloid milling) techniques was shown to be the most efficient for producing EFV nanosuspensions. This resulted in dried nanocrystals with high and fast dissolution profiles. Another advantage of this method is that the drug concentration (drug load) was higher than those presented by other studies referenced previously. This is important since the drug load is directly related to the yield of the process.

Performing studies to comprehend the EFV crystallization process could provide insight into the reason why some of the presented results were not in agreement with the literature. Scale-up studies will be

required to adapt the viscosity issue of the suspensions to the production point of view. Many aspects are still open for study, such as EFV tablet compression and nanocrystal performance in vivo.

REFERENCES

- Alves LDS, De La Roca Soares MF, Albuquerque CT, Silva, ER, Vieira ACC, Fontes DAF, et al. Solid dispersion of efavirenz in pvp k-30 by conventional solvent and kneading methods. *Carbohydr Polym.* 2014;104:166-74.
- Beck C, Dalvi SV, Dave RN. Controlled Liquid Antisolvent Precipitation Using a Rapid Mixing Device. *Chem Eng Sci.* 2010, 65(21):5669-75.
- Blachère JR, Brittain HG. X-Ray Diffraction Methods for the Characterization of Solid Pharmaceutical Materials. In: Adeyeye M, Brittain HG, editor. *Drugs and Pharmaceutical Sciences: Preformulation in Solid Dosage Form Development*. 1st ed. New York: Informa Healthcare. 2008. p. 229-52.
- BRASIL. Farmacopéia Brasileira. 5^a. ed. [s.l.] Agência Nacional de Vigilância Sanitária - ANVISA, 2010.
- Burger D, van der Heiden I, la Porte C, van der Ende M, Groeneveld P, Richter C, et al. Interpatient variability in the pharmacokinetics of the hiv non-nucleoside reverse transcriptase inhibitor efavirenz: the effect of gender, race, and CYP2B6 polymorphism. *Br J Clin Pharmacol.* 2006;61(2):148-54.
- Carstensen JT, *Drugs and the Pharmaceutical Sciences: Advanced Pharmaceutical Solids*. 1st ed. New York: Marcel Dekker, Inc. 2001.
- Chadha R, Poonam A, Anupam S, Jain DS. An Insight into thermodynamic relationship between polymorphic forms of efavirenz. *J Pharm Pharm Sci.* 2012;15(2):234-51.
- Chiappetta DA, Hocht C, Taira C, Sosnik A. Oral pharmacokinetics of the Anti-HIV efavirenz encapsulated within polymeric micelles. *Biomaterials.* 2010;32(9):2379-87.
- Cho E, Cho W, Cha KH, Park J, Kim MS, Kim JS, et al. Enhanced dissolution of megestrol acetate microcrystals prepared by antisolvent precipitation process using hydrophilic additives. *Int J Pharm.* 2010;396(1-2):91-98.
- Comba S, Sethi R. Stabilization of highly concentrated suspensions of iron nanoparticles using shear-thinning gels of xanthan gum. *Water Res.* 2009;43(15):3717-26.
- da Costa MA, Lione VOF, Rodrigues CR, Cabral LM, Rocha HVA. Efavirenz dissolution enhancement II: aqueous co-spray-drying. *Int J Pharm Sci Res.* 2015;6(9):3807-20.
- da Costa MA, Seicera RC, Rodrigues CR, Hoffmeister CRD, Cabral LM, Rocha HVA, et al. Efavirenz dissolution enhancement I: Co-Micronization. *Pharmaceutics.* 2013;5(1):1-22.
- Cristofoletti R, Nair A, Abrahamsson B, Groot DW, Kopp S, Langguth P, et al. Biowaiver monographs for immediate release solid oral dosage forms: efavirenz. *J Pharm Biomed Anal.* 2013;102(2):318-29.
- Fandaruff C, Rauber GS, Araya-sibaja AM, Pereira RN, Campos CEM, Rocha HVA, et al. Polymorphism of Anti-HIV drug efavirenz : investigations on thermodynamic and dissolution properties. *Cryst Growth Des.* 2014;14:4968-75.
- Flint EB, Suslick KS. The Temperature of cavitation. *Science.* 1991;253(5026):1397-99.
- Gao L, Liu G, Ma J, Wang X, Zhou L, Li X, et al. Drug nanocrystals: in vivo performances. *J Control Release.* 2012;160(3):418-30.
- Gao L, Liu G, Ma J, Wang X, Zhou L, Li X, et al. Application of drug nanocrystal technologies on oral drug delivery of poorly soluble drugs. *Pharm Res.* 2013;30(2):307-24.
- Gomes ECL, Mussel WN, Resende JM, Fialho SL, Barbosa J, Yoshida MI. Chemical interactions study of antiretroviral drugs efavirenz and lamivudine concerning the development of stable fixed-dose combination formulations for AIDS treatment. *J Braz Chem Soc.* 2013;24(4):573-79.
- Hoffmeister C, Fandaruff C, Costa M, Cabral L, Pitta L, Bilatto S, et al. Efavirenz dissolution enhancement iii: colloid milling, pharmacokinetics and electronic tongue evaluation. *Eur J Pharm Sci.* 2017;99:310-17.
- Jain S, Sharma JM, Agrawal AK, Mahajan RR. Surface stabilized efavirenz nanoparticles for oral bioavailability enhancement. *J Biomed Nanotechnol.* 2013;9(11):1862-74.
- Khadka P, Ro J, Kim H, Kim I, Kim JT, Kim H, et al. ScienceDirect *Pharmaceutical Particle Technologies : An Approach to Improve Drug Solubility, Dissolution and Bioavailability.* Asian J Pharm. 2014;1-13.
- Laot CM. Spectroscopic characterization of molecular interdiffusion at a poly(vinyl pyrrolidone)/vinyl ester interface. [Master's dissertation] Blacksburg: Virginia Polytechnic Institute and State University, 1997.
- Lee J, Cheng Y. Critical Freezing Rate in Freeze Drying Nanocrystal Dispersions. *J Controlled Release.* 2006;111(1-2):185-92.
- Liu G, Zhang D, Jiao Y, Zheng D, Liu Y, Duan C, et al. Comparison of different methods for preparation of a Stable Riccardin D Formulation via nano-technology. *Int J Pharm.* 2012;422(1-2):516-22.

- Mahapatra S, Thakur TS, Joseph S, Varughese S, Desiraju GR. New solid state forms of the Anti-HIV drug efavirenz. Conformational flexibility and High Z' Issues. *Cryst Growth Des.* 2010;10(7):3191-32.
- Matteucci ME, Hotze MA, Johnston KP, Williams RO. Drug nanoparticles by antisolvent precipitation: mixing energy versus surfactant stabilization. *Langmuir.* 2006;22(21):8951-59.
- Muller RH, Keck CM. Challenges and solutions for the delivery of biotech drugs--a review of drug nanocrystal technology and lipid nanoparticles. *J Biotechnol.* 2004;113(1-3):151-70.
- Nickerson B, Joseph R, Palmer C, Opio A, Beresford G. Analytical method development: Challenges and solutions for low-dose oral dosage forms. In: Zheng J, editor. *Formulation and Analytical Development for Low-Dose Oral Drug Products* 1st ed. Hoboken: Wiley, 2009. p. 241-264.
- Patel AP, Patel JK, Patel KS, Deshmukh AB, Mishra BR. A review on drug nanocrystal a carrier free drug delivery. *Int J Res Ayurveda Pharm.* 2011;2(2):448-58.
- Patel GV, Patel VB, Pathak A, Rajput SJ. Nanosuspension of efavirenz for improved oral bioavailability: formulation optimization, in vitro, in situ and in vivo evaluation. *Drug Dev Ind Pharm.* 2014;40(1):80-91.
- Peltonen L, Hirvonen J. Pharmaceutical nanocrystals by nanomilling: critical process parameters, particle fracturing and stabilization methods. *J Pharm Pharmacol.* 2010;62(11):1569-79.
- Salazar J, Ghanem A, Müller RH, Möschwitzer JP. Nanocrystals: comparison of the size reduction effectiveness of a novel combinative method with conventional top-down approaches. *Eur J Pharm Biopharm.* 2012;81(1):82-90.
- Sartori GJ, Prado LD, Rocha HVA. Efavirenz dissolution enhancement iv—antisolvent nanocrystallization by sonication, physical stability, and dissolution. *AAPS PharmSciTech.* 2017;18(8):3011-3020.
- Savjani KT, Gajjar AK, Savjani JK. Drug solubility : importance and enhancement techniques. *ISRN Pharmaceutics.* 2012;2012:1-10.
- Sawant SV, Kadam VJ, Jadhav KR, Sankpal SV. Drug Nanocrystals: novel technique for delivery of poorly soluble drugs. I. *J Sci Innov Disc.* 2011;1(3):1-15.
- Shankar S, Rhim J. Preparation of nanocellulose from micro-crystalline cellulose: the effect on the performance and properties of agar-based composite Films. *Carbohydr Polym.* 2016;135:18-26.
- Sinha B, Müller RH, Möschwitzer JP. Bottom-up approaches for preparing drug nanocrystals: formulations and factors affecting particle Size. *Int J Pharm.* 2013a;453(1):126-41.
- Sinha B, Müller RH, Möschwitzer JP. Systematic investigation of the cavi-precipitation process for the production of ibuprofen nanocrystals. *Int J Pharm.* 2013b;458(2):315-23.
- Stuart B. *Infrared Spectroscopy: Fundamentals and Applications.* Hoboken: J. Wiley, 2004.
- Sze A, Erickson D, Ren L, Li D. Zeta-potential measurement using the smoluchowski equation and the slope of the current-time relationship in electroosmotic flow. *J Colloid Interface Sci.* 2003;261(2):402-10.
- Theophile T. *Infrared Spectroscopy - Materials science, engineering and technology.* London: InTechOpen. 2012.
- Tung HH, Paul E, Midler M, McCauley JA. *Crystallization of organic compounds: an industrial perspective.* Hoboken: Wiley. 2008.
- Verma S, Gokhale R, Burgess DJ. A Comparative study of top-down and bottom-up approaches for the preparation of micro/nanosuspensions. *Int J Pharm.* 2009;380(1-2):216-22.
- de Waard H, Grasmeijer N, Hinrichs WLJ, Eissens AC, Pfaffenbach PPF, Frijlink HW. Preparation of drug nanocrystals by controlled crystallization: application of a 3-way nozzle to prevent premature crystallization for large scale production. *Eur J Pharm Sci.* 2009;38(3):224-29.
- Wu L, Zhang J, Watanabe W. Physical and chemical stability of drug nanoparticles. *Adv Drug Deliv Rev.* 2011;63(6):456-69.
- Yang L, Chu D, Wang L, Ge G, Sun H. Facile synthesis of porous flower-like srco3 nanostructures by integrating bottom-up and top-down routes. *Mater Lett.* 2016;167:4-8.
- Ye X, Patil H, Feng X, Tiwari RV, Lu J, Gryczke A, et al. Conjugation of hot-melt extrusion with high-pressure homogenization: a novel method of continuously preparing nanocrystal solid dispersions. *AAPS PharmSciTech* 2015;17(1):78-88.
- Zhao H, Wang JX, Wang QA, Chen JF, Yun J. Controlled liquid antisolvent precipitation of hydrophobic pharmaceutical nanoparticles in a microchannel Reactor. *Ind Eng Chem Res.* 2007;46(24):8229-35.

Received for publication on 09th October 2019

Accepted for publication on 18th April 2019